Stefan BROCK

Poznań University of Technology

Hybrid P–PI sliding mode position and speed controller for variable inertia drive

Abstract. *Control system for a variable inertia drive based on a hybrid P–PI sliding mode controller and reference trajectory generator is described in this paper. Sliding mode block with boundary layer (active for large error values) and the P–PI block (active for small error values) are combined in one controller. Simulation results show that this control approach can decrease tracking error, enhance system robustness and attenuate high frequency chattering in the control signal. The results of simulation are confirmed by experimental studies.*

Streszczenie. *W artykule przedstawiono układ sterowania dla napędu o zmiennej bezwładności. W układzie tym zaproponowano generator trajektorii wzorcowej oraz hybrydowy regulator położenia i prędkości. W regulatorze połączono blok regulatora ślizgowego z warstwą graniczną (aktywny dla dużych wartości uchybu) z blokiem P–PI (aktywnym dla małych wartości uchybu). Badania symulacyjne wykazały, że takie podejście zmniejsza błędy śledzenia, poprawia odporność i eliminuje szybkie oscylacje sygnału sterującego. Badania eksperymentalne potwierdziły wyniki.* ***(Hybrydowy P–PI – ślizgowy regulator położenia i prędkości dla napędu o zmiennej bezwładności)***

Keywords: robust control, sliding mode control, hybrid controller, direct drive.
Słowa kluczowe: sterowanie odporne, sterowanie ślizgowe, regulator hybrydowy, napęd bezpośredni.

doi:10.12915/pe.2014.05.06

Introduction

Drive systems of industrial robots and Computer Numerical Controlled (CNC) machines have to meet high requirements of its dynamic properties. One of the important requirements is robustness of the control system. Robustness is defined as the ability of a closed-loop control system to maintain certain dynamic parameters despite the uncertainty of controlled system modeling and external disturbances. Robustness of the drives for each machine axis or industrial manipulator joint is necessary in order to eliminate the interaction of drives and to minimize reference trajectory motion errors. An important parameter with a wide range of variation is the moment of inertia of the drive. For example, it is dependent on the weight of the work piece in the machine, or on the relative configuration of the industrial manipulator arms.

Position control systems operate in general with interpolation blocks, in which the reference position is determined by the reference trajectory. In many industrial servodrive applications, the reference position may be changed during the motion. These changes, caused by the movement of the processing object or by an access to additional information during positioning process, require modifications in the current reference position trajectory. The designated movement trajectory should be described in such a way that it is possible to faithfully track by the drive. This means that not only maximum speed, but also acceleration and jerk (the time derivative of acceleration) need to be limited simultaneously. On-line determination of a new trajectory on the basis of current motion parameters (momentary position, speed, acceleration, jerk), the setpoint value and imposed restrictions is essential in order to perform this task [1]. In the article a new proposal of a suitable reference trajectory generator is used [2, 3].

Sliding mode controllers are widely used in automation systems of electric drive [4, 5, 6]. They provide control system robustness to limited change of parameters, modeling errors and disturbances. However, direct application of the sliding mode control law for the synthesis of position and speed controller lead to rapid changes of the control signal (chattering). Various modifications of the control law are proposed, for example: the use of a continuous saturation function instead of discrete switching block in the controller, or the appropriate filtering of the control signal. In this study a continuous approximation of the switching function was also used.

Good control properties of classical P and PI controllers and robustness of the sliding mode controller are the basis of many works aimed at construction of the hybrid structure, combining advantages of both types of controllers [7, 8, 9].

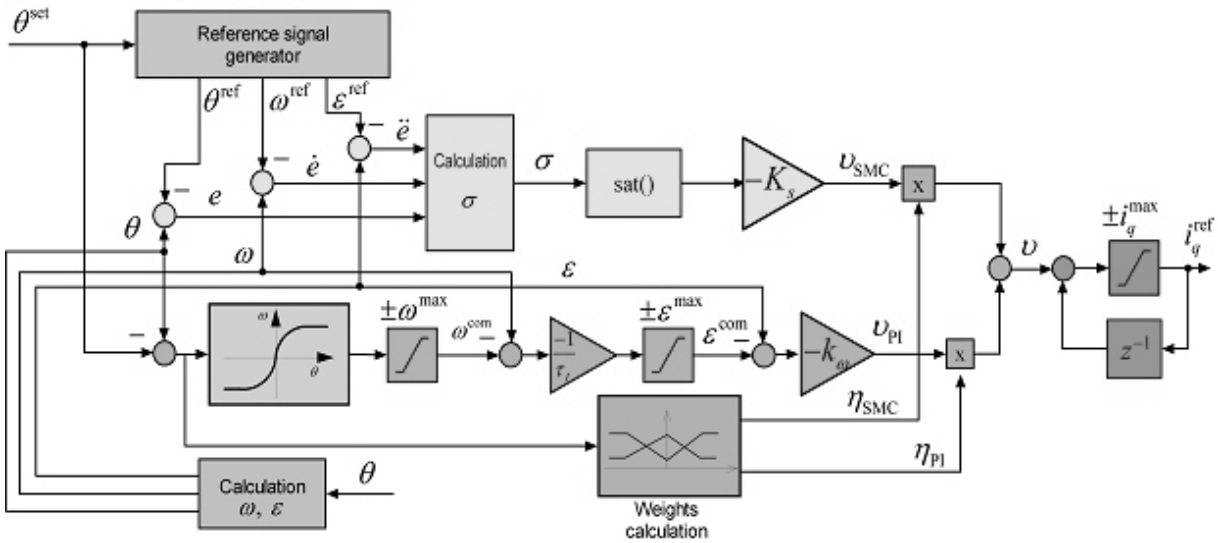

Fig. 1. Block diagram of proposed hybrid PI sliding mode controller

Different parallel structures, in which the control output signal is obtained as a result of the aggregation of individual signals from the controllers, have been widely described in the last years. One of the controllers is selected by the decision-making block depending on current work conditions – in the transient state the sliding mode controller is chosen, in surrounding of the steady-state – the PI controller is selected. The use of fuzzy inference block to aggregate control signals is proposed by some authors. In the work a similar approach, well suited for implementation in the real time control system, was used.

The remaining part of the article is organized as follows: in the section 2 the proposed hybrid structure of position and speed controller are shown, in the section 3 the laboratory stand is presented. The results of simulation and laboratory tests are given in section 4. The summary and final remarks can be found in section 5.

The structure of the hybrid position and speed controller

The proposed structure of the hybrid position and speed controller is presented in Figure 1. On the block diagram the following components of the hybrid controller are shown: reference signal generator, module of the sliding mode controller, module of the cascade P-PI position and speed controller, block of signals aggregation and signal weights determination and the output integrator.

The non-linear position controller block is fed by position error signal e_θ, determined according to the formula:

(1) $$e_\theta = \theta - \theta^{\text{set}}$$

where θ is the momentary position value , while θ^{set} is the reference position value. Output signal of the position controller block is a command speed ω^{com} defined by a relationship:

(2) $$\omega^{\text{com}} = -\min\left(\left|k_\theta \cdot e_\theta\right|, \sqrt{2 \cdot \varepsilon^{\max} \cdot e_\theta}\right) \cdot \text{sgn}(e_\theta)$$

where k_θ is the value of the proportional gain of the position controller, while $\varepsilon^{\max}$ describes the maximum permissible acceleration, allowed in all load conditions. The value of the proportional gain of the position controller is derived from the conditions of the aperiodic response of a closed-loop system, and is dependent on the range of variability of the drive parameters specified in the project and assumed summary delays in the loop. The issue of the selection of controllers parameters was more widely presented in [10, 11].

The difference between the value of command speed ω^{com} and calculated actual speed ω determines speed error, which speed controller is fed with:

(3) $$e_\omega = \omega - \omega^{\text{com}}$$

The output signal of the speed controller is a reference current i_q^{ref}, in accordance with the formula:

(4) $$i_q^{\text{ref}} = -k_\omega \cdot \left(e_\omega + \frac{1}{\tau_I} \int_0^t e_\omega \mathrm{d}\xi \right)$$

where k_ω and τ_I are gain and integration time of the proportional-integral controller respectively. PI speed controller can be presented as a cascading combination of proportional speed controller and integrating acceleration controller. Command acceleration ε^{com} is determined as:

(5) $$\varepsilon^{\text{com}} = -\frac{1}{\tau_I} \cdot e_\omega$$

and then the acceleration error e_ε

(6) $$e_\varepsilon = \varepsilon - \varepsilon^{\text{com}}$$

and the output signal i_q^{ref} are calculated

(7) $$i_q^{\text{ref}} = -k_\omega \cdot \int_0^t e_\varepsilon \mathrm{d}\xi = \int_0^t \upsilon_{PI} \mathrm{d}\xi$$

where υ_{PI} describes the signal feeding the final integrator of the controller. This representation describes the PD-I controller structure often used in practice, wherein only the feedback signal is differentiated in the PD part. In the applied structure it is easy to take into account limiting motion parameters: the maximum speed and the maximum acceleration. For the simplification limits were omitted in the presented equations (1)–(7).

The start point for the synthesis of the sliding mode controller is to define the sliding surface in the space of position error and position error derivatives. For the sliding mode controller it is assumed that the position error is defined as the difference between the actual position θ and the reference value θ^{ref}:

(8) $$e = \theta - \theta^{\text{ref}}$$

First and second time derivative of the position error are defined similarly, on the basis of the reference speed ω^{ref} and reference acceleration ε^{ref} respectively.

(9) $$\dot{e} = \omega - \omega^{\text{ref}}$$

(10) $$\ddot{e} = \varepsilon - \varepsilon^{\text{ref}}$$

The sliding surface is the locus in the space of position error and position error derivatives, in which the generalized error σ is equal to 0.

(11) $$\sigma = \ddot{e} + 2 \cdot \lambda \cdot \dot{e} + \lambda^2 \cdot e$$

During the sliding motion the generalized error disappears with a time constant $1/\lambda$. The output signal from the sliding mode control block υ_{SMC} tends to bring the state vector in error space to the sliding surface, and next to hold on this surface.

(12) $$\upsilon_{SMC} = -K_s \cdot \text{sgn}(\sigma) \qquad \text{sgn}(\sigma) = \begin{cases} -1 & \text{dla} \quad \sigma < 0 \\ 0 & \text{dla} \quad \sigma = 0 \\ 1 & \text{dla} \quad \sigma > 1 \end{cases}$$

The constant K_s is chosen to ensure a stable operation in the whole range of changes of the object parameters. The output signal of the sliding mode control block υ_{SMC} is the first derivative of the reference active current values i_q^{ref}

(13) $$i_q^{\text{ref}} = \int_0^t \upsilon_{SMC} \mathrm{d}\xi$$

In the presented configuration of the sliding mode controller with output integrator the phenomenon of rapid change-over control signal (chattering phenomenon) does not occur. In addition, signum function $\text{sgn}()$ is replaced by a continuous approximation function $\text{sat}()$ with a width equal to Φ

$$\upsilon_{SMC} = -K_s \cdot \mathrm{sat}(\sigma)$$

(14)
$$\mathrm{sat}(\sigma) = \begin{cases} \sigma / \Phi & \text{dla} \quad |\sigma| < \Phi \\ \mathrm{sgn}(\sigma) & \text{dla} \quad |\sigma| \geq \Phi \end{cases}$$

Analysis of the block diagram in Figure 1 shows that the structures of both controller modules are similar. Therefore it is possible to connect their output signals. Due to the need of limit the reference current signal, it is useful to perform an aggregation before a block of an integrator. The reference current value is described with equation:

(15)
$$i_q^{\mathrm{ref}} = \int_0^t \left(\eta_{SMC} \cdot \upsilon_{SMC} + \eta_{PI} \cdot \upsilon_{PI}\right) \mathrm{d}\xi$$

where η_{SMC} and η_{PI} are the weights of the sliding mode component and the PI controller component respectively. Weight value can be chosen arbitrarily, or changed depending on position error values. In the work [7] use a simple fuzzy inference system was suggested, described by the following rule base:

IF error is small **then** PI controller action is dominating

IF error is large **then** SMC action is dominating

For the purposes of the implementation in the real time it is important to minimize the computational complexity of the algorithm. In this case, the fuzzy inference block may be replaced by a simple weight selection rules.

(16)
$$\eta_{SMC} = \min\left(\frac{|e|}{e^{\max}} \cdot \left(\eta^{\max} - \eta^{\min}\right) + \eta^{\min},\ \eta^{\max}\right)$$
$$\eta_{PI} = \max\left(\eta^{\max} - \frac{|e|}{e^{\max}} \cdot \left(\eta^{\max} - \eta^{\min}\right),\ \eta^{\min}\right)$$

where $\eta^{\min}$ and $\eta^{\max}$, describe the range of variation of weights for position error within $<-e^{\max}, e^{\max}>$ interval, respectively. For a given definition the sum satisfies the equation $\eta_{SMC} + \eta_{PI} = \eta^{\min} + \eta^{\max}$. In the paper, on the basis of the tests, arbitrarily values were assumed $\eta^{\min} = 0.3$ and $\eta^{\max} = 0.7$ whereas $e^{\max} = 20$ mrad. In the Figure 2 the characteristics of the weights as a function of position error is shown.

Reference signal generator based on the variable set-point position θ^{set} determines suboptimal time waveforms: reference position θ^{ref}, reference speed ω^{ref} and reference acceleration $\varepsilon^{\mathrm{ref}}$. Examples of reference waveforms corresponding to the step change of set-point position θ^{set} are shown in the Figure 3. In this case the reference waveforms consist of six phases:

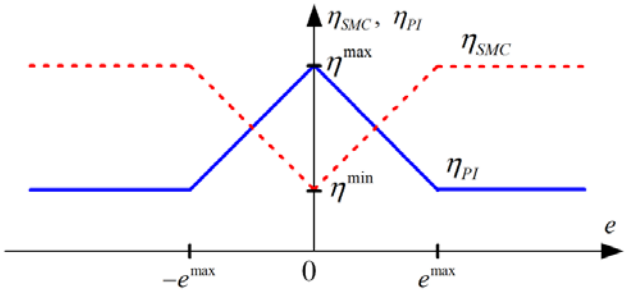

Fig. 2 Characteristics of the weights as a function of position error

increasing acceleration with a limited jerk (A), constant acceleration (B), continuous change of acceleration down to negative value (C), constant delay (D), optimal time deceleration (E), and final phase of the exponential deceleration (F), ensuring operation without overshoot. In the case of larger step change of set-point position, an additional phase occurs during the motion at a constant speed.

Reference signal generator is built based on the idealized model of the drive system with speed and position control loops. An accurate description of the structure and selection of parameters are presented in the works [2, 3].

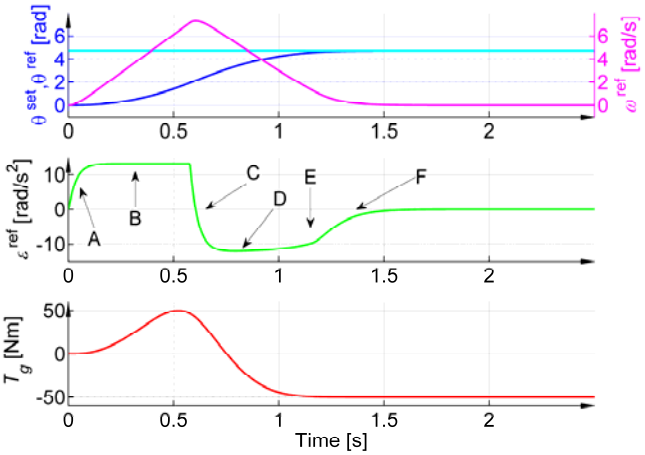

Fig. 3. References signals: top: actual position (blue), reference position (cyan) and reference speed (magenta); middle: reference acceleration; bottom: gravitation torque.

Laboratory stand

Laboratory tests were carried out on a laboratory stand equipped with direct drive permanent magnet synchronous motor (PMSM). In the Figure 4 the functional diagram of the laboratory stand, described accurately at previous works, is shown [12-14]. The motor is loaded with a mechanical set, consisting of inertia plates mounted on an arm on both sides of the shaft and a brake disc with friction clamps. The motor is powered by a voltage source inverter with PWM and controlled by the a DSP controller. The task of vector control with fast PI controllers of active and reactive current components is performed by implemented software. The signal of the command active current is determined by the analyzed in the work position and speed controller. Actual position of the motor shaft is measured using a rotary encoder, and using this signal the value of actual speed is calculated. For the elimination of resonant vibration of mechanical set an additional digital filtration was applied in the speed calculation path [15, 16].

Identified parameters of the laboratory stand were used for synthesis of a simulation model of the whole drive system, including control loops.

Results of simulation and laboratory studies.

Tests have been carried out in two stages: simulation studies and laboratory verification tests. During the simulation, it was assessed whether the introduction of the hybrid controller with the sliding mode block improves the quality of the control process in comparison to the P-PI controller. In the Figures 5 to 7 tracking errors of the drive reference trajectory are shown for the three analyzed cases: small, medium, and large moment of inertia. In the case of medium moment of inertia the system is also affected by an additional gravitational load torque. The

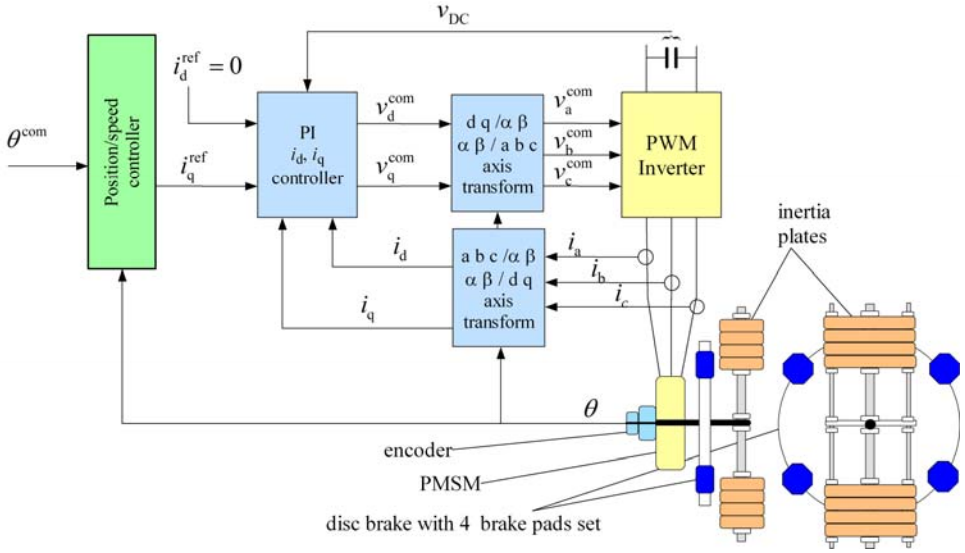

Fig. 4. Block diagram of laboratory stand with a vector-controlled PMSM direct drive

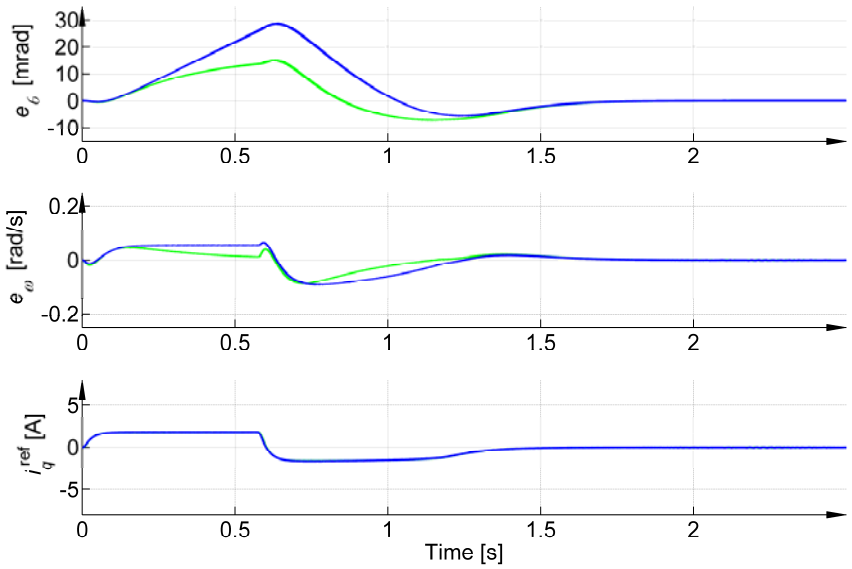

Fig. 5. Comparison of PI (blue line) and hybrid (green line) controllers. Small inertia case. Top: position error, middle: speed error, bottom: reference current. Simulations results.

studied test consisted in the step change of the set-point position of 4.71 rad (0.75 revolution). Reference position, reference speed and reference acceleration waveforms are shown in Figure 3. In addition, in this figure the load torque waveform T_g is also shown. In the drawings 5 to 7 the position error e_θ, speed error e_ω and command signal of active current component i_q^{ref} are presented. In all cases, the introduction of hybrid controller reduced the reference trajectory tracking errors. Fast oscillations does not appear in the command signal of active current component.

At the second stage of the research a laboratory verification was carried out. Summary results are presented in the Figure 8. Waveforms of position and speed (upper chart), the position error relative to the reference position (middle chart) and the command signal of active current component (lower chart) were registered for four cases: small inertia, medium inertia with gravity load torque, large inertia, and additionally small inertia with high dry frictional load torque. The results obtained in laboratory confirm the wavewforms obtained in simulation studies and differences occur only in the final stage of the positioning. Therefore error waveforms were much zoomed on the middle chart. In the case without frictional load torque the final positioning error is smaller than 0.1 mrad, and only in the case of frictional load torque the final positioning error increases to 0.2 mrad (useful resolution of measurement position was 0.05 mrad). Small oscillations of the command active current component (visible especially for the case of a small inertia) arise due to incomplete suppressing of resonant mechanical system

Conclusion

The proposed hybrid position and speed controller is characterized by good dynamic properties and robustness to changes of the parameters. The use of the reference trajectory generator makes it possible to define the tracking error, and then design a sliding surface for a sliding mode controller block. Application of the control system structure with integrating output block has enabled a simple aggregation of the output signals of controller modules.

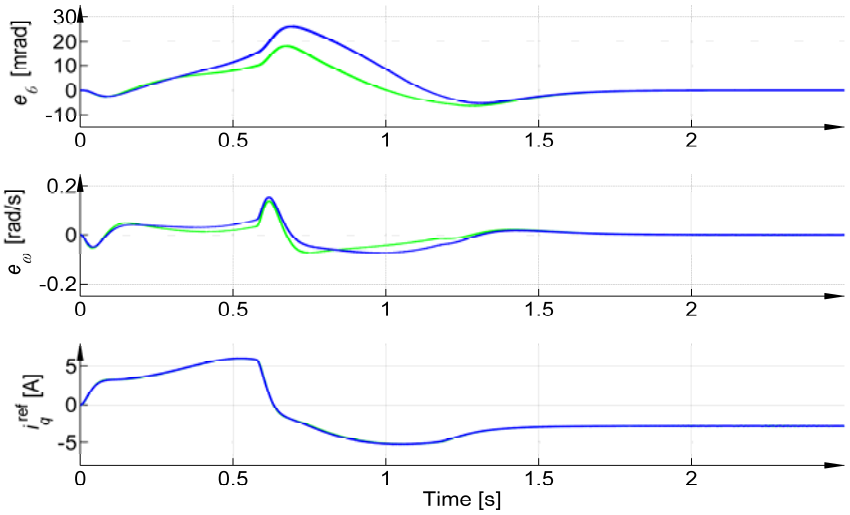

Fig. 6. Comparison of PI (blue line) and hybrid (green line) controllers. Middle inertia case, large gravity load torque. Top: position error, middle: speed error, bottom: reference current. Simulations results

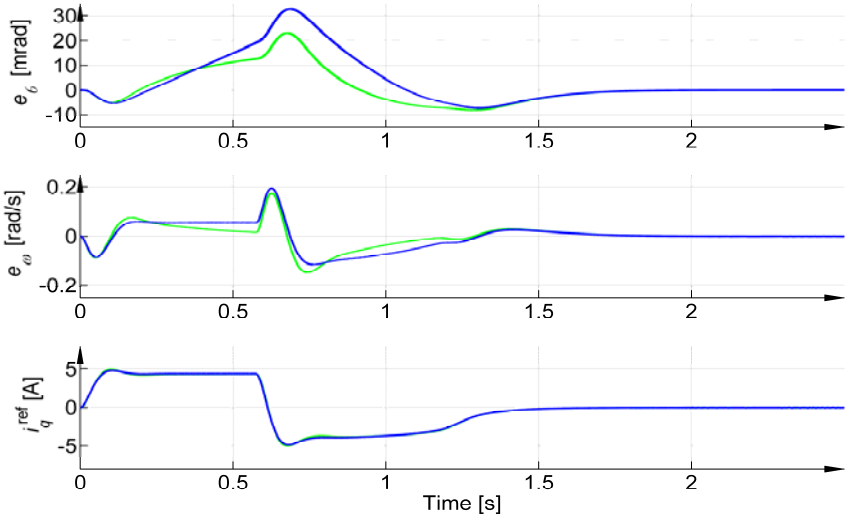

Fig. 7. Comparison of PI (blue line) and hybrid (green line) controllers. Large inertia case. Top: position error, middle: speed error, bottom: reference current. Simulations results

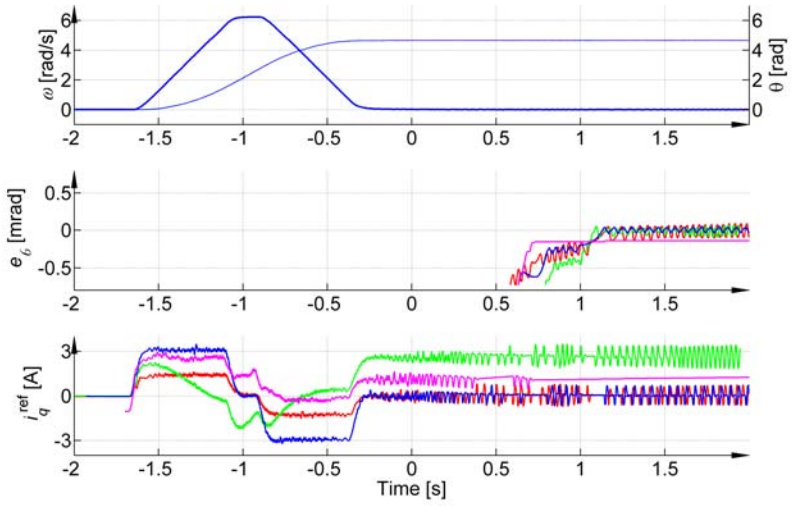

Fig. 8. Robustness of drive with proposed hybrid controller. Top: position and speed, middle: position error, bottom: reference current. Small inertia case (red line), middle inertia case with load torque (green line), large inertia case (blue line), small inertia with friction case (magenta). Experimental results

Proposed in the literature fuzzy inference system has been replaced by a simple weighted sum of the block. In the case of large dry friction torque a small position error occurs, which should be eliminated by further modifying the control law [13].

Appendix. Data of investigated drive

Parameters of PMSM	**Unit**	**Value**
Minimum moment of inertia	$kg \cdot m^2$	0.75
Maximum moment of inertia	$kg \cdot m^2$	5.83
Torque constant	N·m/A	17.5
Rated load torque	N·m	50
Rated value of speed	rad/s	15.1
Rated current in q axis	A	2.85
Rated voltage	V	310

REFERENCES

[1] Kroger, T.: Online Trajectory Generation: Straight-Line Trajectories. *IEEE Transactions on Robotics*. 27 (2011), n.5, 1010–1016.

[2] Brock, S.: Robust position control for direct drive by integral sliding mode controller with reference trajectory generator, *The Symposium on Electromagnetic Phenomena in Nonlinear Circuits* (2012), Pula, Croatia.

[3] Brock S.: Struktury odpornego sterowania elektrycznego napędu bezpośredniego z wykorzystaniem koncepcji sterowania ślizgowego, *Wydawnictwo Politechniki Poznańskiej* (2013)

[4] Sabanovic, A.: Variable Structure Systems With Sliding Modes in Motion Control - A Survey. *IEEE Transaction on Industrial Informatics,* 7 (2011), n.2, 212–223

[5] Orlowska-Kowalska, T., Kaminski, M., Szabat, K.: Implementation of a Sliding–Mode Controller With an Integral Function and Fuzzy Gain Value for the Electrical Drive With an Elastic Joint., *IEEE Transactions on Industrial Electronics*, 57 (2010), n.4, 1309–1317.

[6] Bartoszewicz, A., Żuk, J., Sliding mode control — Basic concepts and current trends. *IEEE International Symposium on Industrial Electronics*. (2010), 3772–3777.

[7] Mohamed, H.A.F., Yang, S.S., Moghavvemi, M.: Improving induction motors speed and flux control using Fuzzy-SMC-PI, *IEEE International Conference on Industrial Technology* (2009), 1–6.

[8] Liu, Z.: Hybrid Speed Control with Sliding-Mode plus Self-Tuning PI for Induction Motor Drive, *49th IEEE International Midwest Symposium on Circuits and Systems* MWSCAS (2006), vol. 1, 500–504.

[9] Abianeh, A.J.: Chattering-free classical variable structure direct torque controlled IPM synchronous motor drive by using PI controller within boundary layer, *6th IEEE Conference on Industrial Electronics and Applications* (2011), 651–656.

[10] Zawirski, K., Deskur, J., Kaczmarek, T.: Automatyka napędu elektrycznego. *Wydawnictwo Politechniki Poznańskiej* (2012)

[11] Brock, S., Deskur, J., Zawirski, K.: Control problems of direct servodrives with PMSM, *Power Electronics and Electrical Drives — Selected Problems*. Polish Academy of Sciences, Electrical Engineering Committee Wrocław (2007), 331–347.

[12] Pajchrowski, T., Zawirski, K.: Synteza odpornego regulatora prędkości wykorzystującego sztuczne sieci neuronowe z silnikiem synchronicznym o magnesach trwałych. *Przegląd Elektrotechniczny (Electrical Review),* 82 (2006), nr 2, 57–61.

[13] Brock, S.: Sliding mode controller for direct drive with dry friction. *Przegląd Elektrotechniczny (Electrical Review)*, 85 (2009),nr 7, 125–129

[14] Brock, S.: Sterowanie ślizgowe napędem bezpośrednim z silnikiem synchronicznym z magnesami trwałymi. *Przegląd Elektrotechniczny (Electrical Review),* (2010) 86, nr 4, 134–137

[15] Szabat, K., Orlowska-Kowalska, T.: Vibration Suppression in a Two-Mass Drive System Using PI Speed Controller and Additional Feedbacks — Comparative Study. *IEEE Transactions on Industrial Electronics,* 54 (2007), n.2, 1193–1206

[16] Brock, S., Łuczak, D.: Speed control in direct drive with non-stiff load. *IEEE International Symposium on Industrial Electronics ISIE* (2011), Gdańsk, Poland, 1937–1942

***Author**: dr inż. Stefan Brock, Poznań University of Technology, Institute of Control and Information Engineering, ul. Piotrowo 3A, 60-965 Poznań, e-mail: Stefan.Brock@put.poznan.pl*